nature physics

LETTERS

PUBLISHED ONLINE: 3 MAY 2009 | DOI: 10.1038/NPHYS1255

High-fidelity transmission of entanglement over a high-loss free-space channel

Alessandro Fedrizzi[1]*, Rupert Ursin[1], Thomas Herbst[1], Matteo Nespoli[1], Robert Prevedel[1,2], Thomas Scheidl[1], Felix Tiefenbacher[1], Thomas Jennewein[1] and Anton Zeilinger[1,2]*

Quantum entanglement enables tasks not possible in classical physics. Many quantum communication protocols[1] require the distribution of entangled states between distant parties. Here, we experimentally demonstrate the successful transmission of an entangled photon pair over a 144 km free-space link. The received entangled states have excellent, noise-limited fidelity, even though they are exposed to extreme attenuation dominated by turbulent atmospheric effects. The total channel loss of 64 dB corresponds to the estimated attenuation regime for a two-photon satellite communication scenario. We confirm that the received two-photon states are still highly entangled by violating the Clauser–Horne–Shimony–Holt inequality by more than five standard deviations. From a fundamental point of view, our results show that the photons are subject to virtually no decoherence during their 0.5-ms-long flight through air, which is encouraging for future worldwide quantum communication scenarios.

Entanglement is at the heart of many peculiarities encountered in quantum mechanics and has enabled many groundbreaking tests on the fundamentals of nature. Entangled photons are ideal tools to investigate the laws of quantum mechanics over long distances and timescales because they are not subject to decoherence. Furthermore, photons can be easily generated, manipulated and transmitted over large distances through optical fibres or free-space links. As the maximal distance for the distribution of quantum entanglement in optical fibres is limited to the order[2–5] of ∼100 km with state-of-the-art technology, the most promising option for testing quantum entanglement on a global scale at present is free-space transmission, ultimately using satellites and ground stations[6].

In recent years, various free-space quantum communication experiments with weak coherent laser pulses[7–11] and entangled photons[12–15] have been carried out on ever larger distance scales and with increasing bit rates. So far, the most advanced test bed for free-space distribution of entanglement is a 144 km free-space link between two Canary Islands, where the successful transmission of one photon of an entangled pair was recently achieved[16]. In the present experiment, we demonstrate a fundamentally more interesting scenario by sending both photons of an entangled pair over this free-space channel. By violating a Clauser–Horne–Shimony–Holt (CHSH) Bell inequality[17], we find that entanglement is highly stable over long time spans—the photon-pair flight time of ∼0.5 ms is the longest lifetime of photonic Bell states reported so far, almost twice as long as the previous high[4,5] of ∼250 μs.

The achieved noise-limited fidelity paves the way for free-space implementations of quantum communication protocols that require the transmission of two photons, such as, quantum dense coding[18], entanglement purification[19], quantum teleportation[20] and quantum key distribution without a shared reference frame[21]. From a technological perspective, the overall two-photon loss bridged in our experiment is significantly higher than the current 40 dB limit[22] for alternative set-ups relying on weak coherent laser pulses. The attenuation of 64 dB corresponds to the expected attenuation for a satellite scenario with two ground stations[6], proving the feasibility of quantum communication on a global scale.

The experiment was conducted between La Palma and Tenerife, two Canary Islands situated in the Atlantic Ocean off the West African coast. An overview of the experimental scheme is shown in Fig. 1. At the transmitter station at La Palma, photon pairs at a wavelength of 810 nm and a bandwidth (full-width at half-maximum) of 0.6 nm were generated in a 10-mm-long, periodically poled $KTiOPO_4$ crystal that was bidirectionally pumped by a grating-stabilized 405 nm diode laser. The photon pairs were coherently combined in a polarization Sagnac interferometer[23,24] and emitted in the maximally entangled state:

$$|\psi\rangle = 1/\sqrt{2}(|HV\rangle + e^{i\varphi}|VH\rangle) \quad (1)$$

where H/V denote the photons polarization state (horizontal/vertical) and φ is an unknown phase.

At 20 mW of pump power, the source produced ∼10^7 photon pairs per second of which ∼3.3×10^6 single photons per second and ∼10^6 pairs per second were detected locally. These pairs were coupled into single-mode fibres with a length difference of 10 m, which introduced a time delay of $\Delta t = 50$ ns between the two photons. The two photons were then transmitted by two telescopes mounted on a motorized platform and a common receiver telescope—the European Space Agency's Optical Ground Station (OGS) located on Tenerife. The transmitters consisted of single-mode fibre couplers and $f/4$ best form lenses (focal length $f = 280$ mm) that had a lateral separation of 10 cm. To actively compensate the transmitter platform and receiver pointing directions for drifts of the optical path through the time-dependent atmosphere, a bidirectional closed-loop tracking mechanism was used: at the transmitter platform, the virtual position of a 532 nm beacon laser attached to the OGS was monitored in the focus of a third telescope by a CCD (charge-coupled device) camera. Likewise, the OGS monitored the position of a beacon laser mounted at the transmitter (see Fig. 1 and ref. 11 for details).

At the OGS, the incoming photons were collected by a 1 m mirror ($f = 38$ m). To ensure that turbulence-induced beam

[1]Institute for Quantum Optics and Quantum Information, Austrian Academy of Sciences, Boltzmanngasse 3, 1090 Vienna, Austria, [2]Quantum Optics, Quantum Nanophysics and Quantum Information, Faculty of Physics, University of Vienna, Boltzmanngasse 5, 1090 Vienna, Austria.
*e-mail: alessandro.fedrizzi@univie.ac.at; zeilinger-office@univie.ac.at.

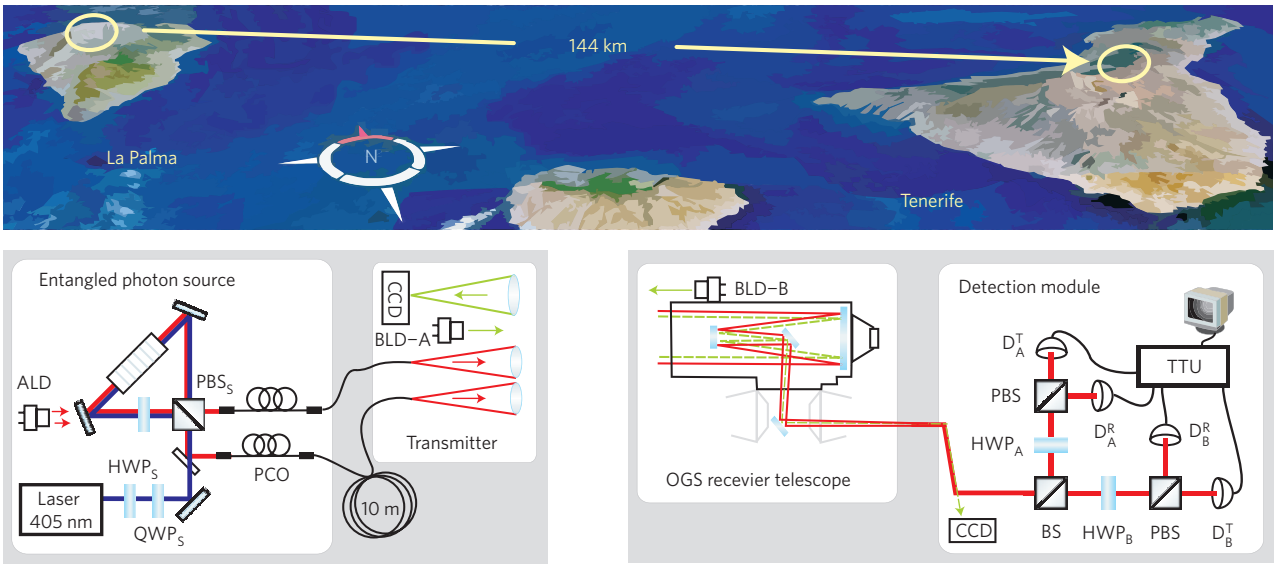

Figure 1 | Satellite image (NASA World Wind) of the Canary Islands of Tenerife and La Palma and overview of the experimental scheme. At La Palma, a Sagnac down-conversion source[24] created narrow-band entangled photon pairs. Manual polarization controllers (PCO) and an auxiliary laser diode (ALD) were used for polarization alignment. The photon pairs were transmitted by a pair of telescopes mounted on a rotatable platform to the 144 km distant receiver (OGS) on Tenerife. The transmitter telescope platform was actively locked to a 532 nm beacon laser diode (BLD-B) attached to the OGS. Likewise, the OGS receiver telescope tracked the virtual position of a 532 nm beacon laser attached to the transmitter (BLD-A). At the OGS, the overlapping photon beams were collected and guided to the detection module by a system of mirrors. This module consisted of a 50/50 beamsplitter cube (BS), and two polarization analysers (A, B). Each of these analysers was formed by one half-wave plate (HWP_A, HWP_B), a polarizing beamsplitter cube (PBS) and two single-photon avalanche photodiodes (D^T_A, D^R_A, D^T_B, D^R_B) placed in the transmitted (T) and the reflected (R) output port of the respective PBS.

wander did not divert the beam off the detectors, the photons were collimated ($f = 400$ mm) before they were guided to a polarization analysis module. Here, a symmetric 50/50 beam splitter directed impinging photons randomly to one of two polarization analysers (A, B), each consisting of a half-wave plate (HWP_A, HWP_B), mounted in a motorized rotation stage, and a polarizing beam splitter (PBS). The polarized light was then refocused ($f = 50$ mm) onto four single-photon avalanche diodes (SPADs). A time-stamping unit recorded clicks in the four SPADs and encoded and stored their respective channel number and arrival time relative to a common internal clock with 156 ps resolution. Figure 2a shows the cross-correlations of these time-stamps for two exemplary measurements. One can clearly identify the two coincidence peaks at ± 50 ns around zero delay, which corresponds to the fibre delay Δt introduced at the transmitter. The average width (full-width at half-maximum) of the coincidence peaks was 560 ps, dominated by the timing jitter of the SPADs. To obtain the number of coincident photons, we summed up the number of correlations in a time window of 1.25 ns centred at the coincidence peak positions (Fig. 2b).

As a witness for the presence of entanglement between the received photons, we tested the CHSH Bell inequality[17]:

$$S(\alpha,\beta,\alpha',\beta') = |E(\alpha,\beta) - E(\alpha,\beta')| + |E(\alpha',\beta') + E(\alpha',\beta)| < 2 \quad (2)$$

where $E(\theta_A,\theta_B) = (C_{TT}(\theta_A,\theta_B) + C_{RR}(\theta_A,\theta_B) - C_{TR}(\theta_A,\theta_B) - C_{RT}(\theta_A,\theta_B))/N$ is the normalized correlation value of polarization measurement results on photon pairs. $C_{ab}(\theta_A,\theta_B)$ is the number of coincidences measured between detectors at the (T/R) output ports (Fig. 1) of the polarization analysers A and B set to angles (θ_A,θ_B) and N is the sum of these coincidences. Whenever S exceeds the classical bound $S > 2$, the polarization correlations cannot be explained by local hidden variable models[17]. For the maximally entangled state $|\psi^-\rangle$, quantum theory predicts a value of $S_{QM} = 2\sqrt{2}$ for the settings $(\alpha,\beta,\alpha',\beta') = (0,\pi/8,\pi/4,3\pi/8)$.

The detection module in our experiment enabled us to directly measure the expectation values $E(\theta_A,\theta_B)$ in equation (2) with four different sets of angles of HWP_A and HWP_B (Table 1). We first aligned the system to obtain a $|\psi^-\rangle$ state at the receiver (see details in the Methods section). For each setting (θ_A,θ_B), we repeatedly accumulated data for typically 900 s, which eventually amounted to a total of 10,800 s acquired in three consecutive nights. Each detector registered an intrinsic dark count rate of $\sim 200\,s^{-1}$, and additionally background light of $\sim 200\,s^{-1}$. In total, we received an average signal of 2,500 single photons per second and 0.071 photon pairs per second. Even though the final single-photon-to-coincidence ratio at the receiver was just 1.7×10^{-5}, the coincidence signal-to-noise ratio was as high as $\sim 15:1$. Compared with the count rates detected at the source, the single-photon attenuation was 34 dB, of which 2 dB was due to the lower efficiency of the detectors used at the receiver ($\sim 25\%$) compared with those at the source ($\sim 40\%$). The measured total photon-pair loss was 71 dB, of which 3 dB was contributed by the beam splitter in the receiver module. The average net attenuation experienced by single photons along the free-space link was therefore 32 dB and the photon-pair attenuation of 64 dB was exactly twice as large, which results from the fact that a pair of photons has double the extinction of a single photon transiting the path. As we have previously ruled out any other adverse effects such as depolarization or timing jitter, which might occur between photons in independent channels[16], we can compare our results to a scenario with two separate free-space links. A detailed analysis[22] of the error sources in our system enabled us to estimate the expected background and multiphoton-pair emissions limited quantum visibility to 94.4%. Combined with the source visibility (99.2%) and the polarization contrast of the detection module (99.5%), the upper bound for the overall system visibility was $V_{tot} = 93.2\%$. As the observed CHSH Bell parameter is connected to the set-up visibility through $S_{max} = V_{tot} \times S_{QM}$, this implies a maximum achievable Bell parameter of $S_{max} = 2.636$.

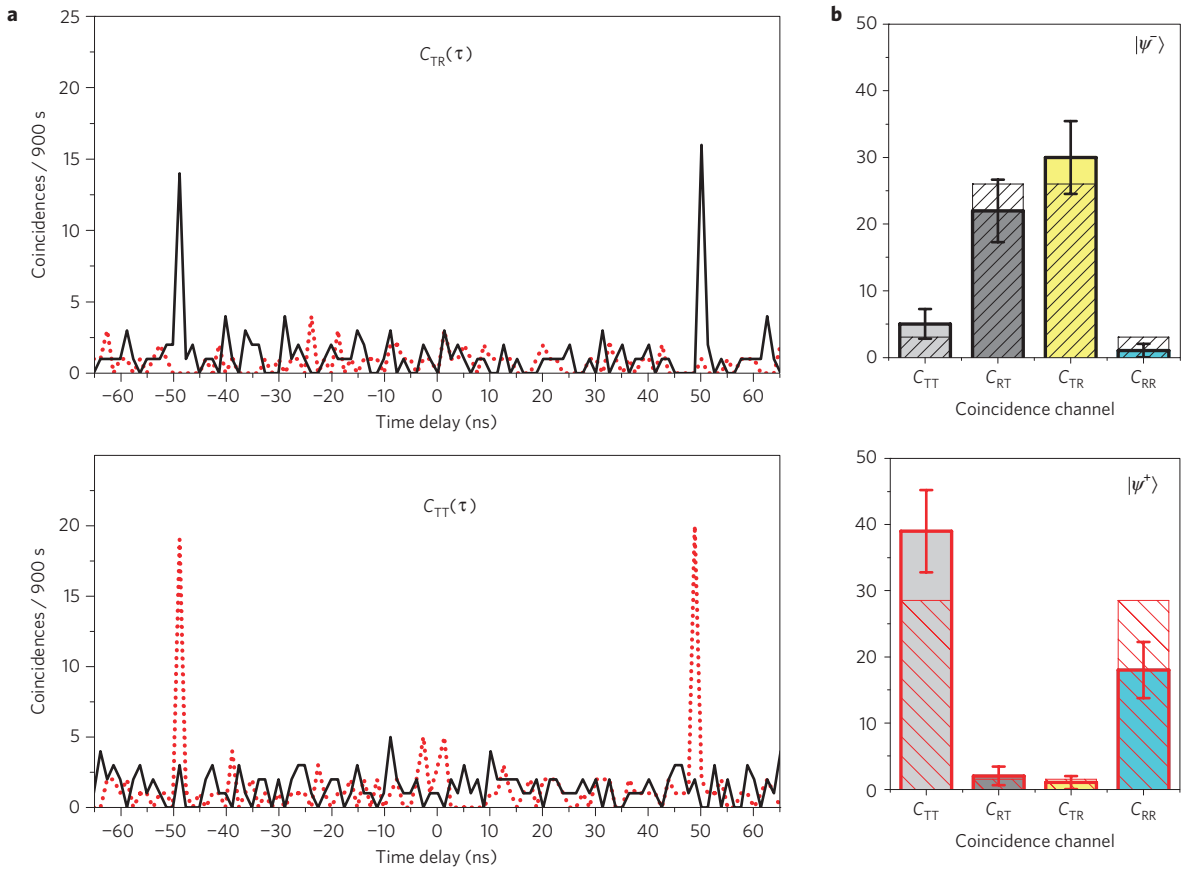

Figure 2 | Coincidence histograms and the respective accumulated coincidence events for measurements on two different Bell states. a, Timing distribution of two out of four coincidence channels. $C_{TR}(\tau)$ and $C_{TT}(\tau)$ between detectors D_A^T-D_B^R (top) and D_A^T-D_B^T (bottom) for a $|\psi^-\rangle$ state (black line) and a $|\psi^+\rangle$ state (dotted red line). The analyser wave plates HWP_A and HWP_B in the detection module were set to $(\pi/8, \pi/8)$. For each detector combination, there are two coincidence peaks at ±50 ns that can be clearly distinguished from the accidental background. **b**, Total coincidence counts and Poissonian standard deviations for all four relevant coincidence channels integrated over a 1.25 ns time window centred at the peak positions. They show distinct $|\psi^-\rangle$ (top) and $|\psi^+\rangle$ (bottom) signatures. The coloured columns show the joint results of the four corresponding detector combinations necessary to fully characterize the state. The hatched columns show the ideal expectation. The accumulation time for each measurement was 900 s.

Table 1 | Experimental polarization correlations $E(\theta_a, \theta_b)$ for the CHSH inequality.

(θ_a, θ_b)	$E(\theta_a, \theta_b)$	$\Delta E(\theta_a, \theta_b)$
$(0, \pi/8)$	−0.604	0.059
$(\pi/4, \pi/8)$	0.672	0.055
$(0, 3\pi/8)$	0.638	0.056
$(\pi/4, 3\pi/8)$	0.697	0.058

The total integration time was 10,800 s. The standard deviations $\Delta E(\theta_a, \theta_b)$ were calculated assuming Poissonian photon count statistics.

The accumulated coincident events for the different detector pairs yielded the correlation values shown in Table 1. According to equation (2), we measured a CHSH Bell parameter S_{exp} of:

$$S_{exp} = 2.612 \pm 0.114$$

which is in excellent agreement with our estimate S_{max}. Our result violates the CHSH inequality by 5.4 standard deviations and convincingly proves the successful transmission of entanglement. The fact that S_{exp} is so close to S_{max} shows that the fidelity between the transmitted and received entangled states was essentially noise-limited. Therefore, the entanglement was not affected by decoherence, even though the photons were subject to extreme attenuation that was dominated by turbulent atmospheric fluctuation[16].

Note that our set-up contains some of the basic building blocks of a quantum communication system. However, the set-up could not be used to carry out an actual quantum key distribution experiment[25] owing to the lack of a second independent analyser module. In addition, a fully-fledged implementation would have required classical post-processing protocols, that is, error correction and privacy amplification. Nevertheless, from the measured S_{exp}, we can infer a qubit error ratio of 3.85 ± 2.2%. Further note that the photon-pair creation rate of ∼10^6 pairs per second at the source is necessary[6] for the long-distance distribution of quantum entanglement in the demonstrated high-attenuation regime. The compact entangled photon source, being pumped by a low-power diode laser, can readily be integrated into a satellite-borne photonic terminal, which was previously[14,16] not the case. We expect that this will enable fundamental tests of the laws of quantum mechanics on a global scale[26].

Methods

Before measuring the polarization correlations for equation (2), we had to establish a common polarization reference frame between the individual transmitters and the receiver and to adjust the phase φ of the quantum state in equation (1) such that the detected coincidence signature was consistent with one of the desired Bell states. For the polarization compensation, we used an auxiliary 808 nm laser diode, which was directed at the entangled source such that linearly polarized light was

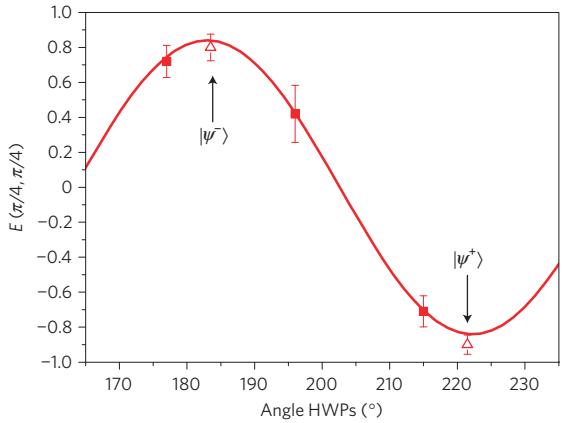

Figure 3 | Scan of the phase φ of the entangled two-photon state in one measurement night. We measured the visibility of the entangled states in the $|\pm\rangle$ basis for three settings of the wave plates controlling the pump laser (squares). After fitting a cosine function ($V_0 = 84 \pm 2.4\%$) to these data points, we were able to adjust the source to emit either $|\psi^-\rangle$ or $|\psi^+\rangle$ states. We prepared these states and observed, in this example, a visibility of $V_\pm = 80 \pm 7.6\%$ for the $|\psi^-\rangle$ and $V_\pm = 90 \pm 5.5\%$ for the $|\psi^+\rangle$ state (triangles). The error bars were determined assuming Poissonian photon count statistics.

coupled into the fibres at a well-defined single-photon level (Fig. 1). We set HWP_A and HWP_B in the detection module to $(0°, 0°)$, measuring in the $|H/V\rangle$ basis, and manually adjusted the fibre polarization controllers at the source to maximize the single-photon polarization visibility $V_{H/V}$ in the remote detectors. The achieved visibility in this basis was typically 95%.

Once the linear polarization was set, the auxiliary laser was switched off and φ was tuned using entangled photons. The visibility $V_\pm$ in the $|\pm\rangle$ basis depends on φ as $V_\pm = V_0 \cos(\varphi)$. To determine the relation between φ and the wave plates controlling the pump laser in the source (HWP_S, QWP_S), we set HWP_A and HWP_B in the detection module to $(\pi/8, \pi/8)$, measured $V_\pm$ for three different settings of HWP_S and QWP_S in the equatorial plane of the Poincaré sphere that represents the pump laser polarization (see refs 23, 24) and then numerically fitted a cosine function to the obtained data points. The fitted two-photon fringes in Fig. 3 correspond to a visibility of $V_0 = 84 \pm 2.4\%$. From this fit, we deduced the wave-plate settings to obtain either a $|\psi^-\rangle$ or a $|\psi^+\rangle$ state in the detection module. This procedure was repeated each night at the beginning of a measurement.

We obtained the coincidence measurements in Fig. 2 after we prepared $|\psi^-\rangle$ and $|\psi^+\rangle$ states using this method. The measured respective visibility of $V_\pm = 80 \pm 7.6\%$ and $V_\pm = 90 \pm 5.5\%$ at the receiver is depicted in Fig. 3. As the linear polarization of the individual photons could be adjusted arbitrarily at the source, we were thus able to prepare, transmit and distinguish any of the four Bell states at the receiver.

Received 7 February 2008; accepted 25 March 2009; published online 3 May 2009

References

1. Gisin, N. & Thew, R. Quantum communication. *Nature Photon.* **1**, 165–171 (2007).
2. Takesue, H. *et al.* Quantum key distribution over a 40-db channel loss using superconducting single-photon detectors. *Nature Photon.* **1**, 343–348 (2007).
3. Hübel, H. *et al.* A high-fidelity transmission of polarization encoded qubits from an entangled source over 100 km of fiber. *Opt. Express* **15**, 7853–7862 (2007).
4. Honjo, T. *et al.* Long-distance distribution of time-bin entangled photon pairs over 100 km using frequency up-conversion detectors. *Opt. Express* **15**, 13957–13964 (2007).
5. Zhang, Q. *et al.* Distribution of time-energy entanglement over 100 km fiber using superconducting single-photon detectors. *Opt. Express* **16**, 5776–5781 (2008).
6. Aspelmeyer, M., Jennewein, T., Pfennigbauer, M., Leeb, W. & Zeilinger, A. Long-distance quantum communication with entangled photons using satellites. *IEEE J. Sel. Top. Quant. Electron.* **9**, 1541–1551 (2003).
7. Kurtsiefer, C. *et al.* A step towards global quantum key distribution. *Nature* **419**, 450 (2002).
8. Buttler, W. T. *et al.* Daylight quantum key distribution over 1.6 km. *Phys. Rev. Lett.* **84**, 5652–5655 (2000).
9. Rarity, J. G., Tapster, P. R. & Gorman, P. M. Secure free-space key exchange to 1.9 km and beyond. *J. Mod. Opt.* **48**, 1887–1901 (2001).
10. Bienfang, J. *et al.* Quantum key distribution with 1.25 Gbps clock synchronization. *Opt. Express* **12**, 2011–2016 (2004).
11. Schmitt-Manderbach, T. *et al.* Experimental demonstration of free-space decoy-state quantum key distribution over 144 km. *Phys. Rev. Lett.* **98**, 10504 (2007).
12. Aspelmeyer, M. *et al.* Long-distance free-space distribution of quantum entanglement. *Science* **301**, 621–623 (2003).
13. Peng, C. *et al.* Experimental free-space distribution of entangled photon pairs over 13 km: Towards satellite-based global quantum communication. *Phys. Rev. Lett.* **94**, 150501 (2005).
14. Resch, K. *et al.* Distributing entanglement and single photons through an intra-city, free-space quantum channel. *Opt. Express* **13**, 202–209 (2005).
15. Marcikic, I., Lamas-Linares, A. & Kurtsiefer, C. Free-space quantum key distribution with entangled photons. *Appl. Phys. Lett.* **89**, 101122 (2006).
16. Ursin, R. *et al.* Entanglement-based quantum communication over 144 km. *Nature Phys.* **3**, 481–486 (2007).
17. Clauser, J., Horne, M., Shimony, A. & Holt, R. Proposed experiment to test local hidden-variable theories. *Phys. Rev. Lett.* **23**, 880–884 (1969).
18. Mattle, K., Weinfurter, H., Kwiat, P. G. & Zeilinger, A. Dense coding in experimental quantum communication. *Phys. Rev. Lett.* **76**, 4656–4659 (1996).
19. Pan, J.-W., Gasparoni, S., Ursin, R., Weihs, G. & Zeilinger, A. Experimental entanglement purification of arbitrary unknown states. *Nature* **423**, 417–422 (2003).
20. Bouwmeester, D., Ekert, A. & Zeilinger, A. *The Physics of Quantum Information: Quantum Cryptography, Quantum Teleportation, Quantum Computation* (Springer, 2001).
21. Boileau, J., Gottesman, D., Laflamme, R., Poulin, D. & Spekkens, R. Robust polarization-based quantum key distribution over a collective-noise channel. *Phys. Rev. Lett.* **92**, 17901 (2004).
22. Ma, X., Fung, C. & Lo, H. Quantum key distribution with entangled photon sources. *Phys. Rev. A* **76**, 12307 (2007).
23. Kim, T., Fiorentino, M. & Wong, F. N. C. Phase-stable source of polarization-entangled photons using a polarization Sagnac interferometer. *Phys. Rev. A* **73**, 12316 (2006).
24. Fedrizzi, A., Herbst, T., Poppe, A., Jennewein, T. & Zeilinger, A. A wavelength-tunable fiber-coupled source of narrowband entangled photons. *Opt. Express* **15**, 15377–15386 (2007).
25. Bennett, C. H., Brassard, G. & Mermin, N. D. Quantum cryptography without Bell's theorem. *Phys. Rev. Lett.* **68**, 557–559 (1992).
26. Armengol, J. M. P. *et al.* Quantum communications at ESA: Towards a space experiment on the ISS. *Acta Astronaut.* **63**, 165–178 (2008).

Acknowledgements

We are grateful to H. Weinfurter, J. G. Rarity, T. Schmitt-Manderbach, C. Barbieri, F. Sanchez, A. Alonso, J. Perdigues and Z. Sodnik, T. Augusteijn and the staff of the Nordic Optical Telescope in La Palma for their support at the trial sites. This work was supported by ESA under the General Studies Programme (No. 18805/04/NL/HE), the European Commission through Project QAP (No. 015846), the DTO-Funded US Army Research Office, the Austrian Science Foundation (FWF) under project number SFB1520 and the ASAP-Programme of the Austrian Space Agency (FFG).

Additional information

Reprints and permissions information is available online at http://npg.nature.com/reprintsandpermissions. Correspondence and requests for materials should be addressed to A.F. or A.Z.